Journal of Hazardous Materials 164 (2009) 18–25

Contents lists available at ScienceDirect

Journal of Hazardous Materials

journal homepage: www.elsevier.com/locate/jhazmat

Design of a neutral electro-Fenton system with Fe@Fe_2O_3/ACF composite cathode for wastewater treatment

Jinpo Li, Zhihui Ai*, Lizhi Zhang

Key Laboratory of Pesticide & Chemical Biology of Ministry of Education, College of Chemistry, Central China Normal University, Wuhan 430079, People's Republic of China

ARTICLE INFO

Article history:
Received 13 January 2008
Received in revised form 12 June 2008
Accepted 25 July 2008
Available online 5 August 2008

Keywords:
Electro-Fenton
Iron
Iron oxide
Core–shell
Neutral pH

ABSTRACT

The narrow pH range limits the wide application of Fenton reaction in the wastewater treatment. It is of great importance to widen working pH range of Fenton reaction from strong acidic condition to neutral, even basic ones. In this study, for the first time nanostructured Fe@Fe_2O_3 was loaded on active carbon fiber (ACF) as an oxygen diffusion cathode to be used in a heterogeneous electro-Fenton (E-Fenton) oxidation system. This novel Fe@Fe_2O_3/ACF composite cathode was characterized by X-ray diffraction (XRD), scanning electron microscopy (SEM), energy dispersive X-ray (EDX) analysis, transmission electron microscopy (TEM), and element mapping. On the degradation of dye pollutant rhodamine B in water, this heterogeneous E-Fenton system with the Fe@Fe_2O_3/ACF cathode showed much higher activity than other E-Fenton systems with commercial zero valent iron powders (Fe^0) and ferrous ions (Fe^{2+}) under neutral pH. On the basis of experimental results, we proposed a possible pathway of rhodamine B degradation in this heterogeneous Fe@Fe_2O_3/ACF E-Fenton process. This heterogeneous E-Fenton system is very promising to remove organic pollutants in water at neutral pH.

1. Introduction

Recently advanced oxidation processes (AOPs) have attracted more and more attention because they can be used to degrade pollutants in water by generating plenty of hydroxyl radicals (•OH) [1–4]. Hydroxyl radicals (•OH) are non-selective, very powerful oxidants. They are able to react with organic pollutants to mineralize these pollutants into CO_2, water and inorganic ions. Fenton reaction is one of the most efficient AOPs [5–9]. It produces •OH through various reactions between ferrous ions and hydrogen peroxide [5,10]. Traditional Fenton reactions with ferrous ions have been employed to efficiently treat a variety of industrial wastewater containing a range of organic compounds like phenols, pesticides, wood preservatives, plastic additives, and rubber chemicals with low cost and relatively easy operation and maintenance [11–14]. However, despite its high efficiency, the wide application of traditional Fenton process is limited by its acidic pH requirement (pH 2–4) and the formation of iron sludge in the coagulation step as well as high cost of hydrogen peroxide.

In order to avoid the use of expensive hydrogen peroxide, electro-Fenton process was established through efficient production of hydroxyl and hydroperoxyl radicals through the reactions between dissolved iron ions and electro-generated H_2O_2 by anodic water oxidation on various anodic electrodes (mercury pool, vitreous carbon or carbon-polytetrafluoroethylene O_2-fed cathodes) and/or O_2 reduction on the cathodal electrodes [15,16]. The hydrogen peroxide formation on the cathodes such as mercury, gold or carbon is realized by the reduction of dissolved oxygen as shown in Eq. (1) [17,18].

$$O_2 + 2H^+ + 2e = H_2O_2 \quad E^0 = \frac{0.69\,V}{NHE} \tag{1}$$

The electro-generated H_2O_2 can then react with dissolved Fe^{2+} to produce •OH through a Fenton process (Eq. (2)).

$$H_2O_2 + Fe^{2+} = Fe(OH)^{2+} + {}^{\bullet}OH \tag{2}$$

The regeneration of Fe^{2+} can occur either by a direct cathodal reaction (Eq. (3)), by the oxidation of an organic (Eq. (4)) or by the reaction with H_2O_2 (Eq. (5)) [19].

$$Fe^{3+} + e^- = Fe^{2+} \tag{3}$$

$$Fe^{3+} + R^{\bullet} = Fe^{2+} + R^+ \tag{4}$$

$$Fe^{3+} + H_2O_2 = [Fe{-}O_2H]^{2+} + H^+ = Fe^{2+} + HO_2{}^{\bullet} \tag{5}$$

Activated carbon fiber (ACF) is an attractive carbon material with excellent characteristics of adsorption, conductivity and catalysis [20]. Because of its large surface area, ACF possesses high adsorption capacity. Meanwhile, its excellent mechanical integrity makes

* Corresponding author. Tel.: +86 27 6786 7535; fax: +86 27 6786 7535.
E-mail address: jennifer.ai@mail.ccnu.edu.cn (Z. Ai).

0304-3894/$ – see front matter © 2008 Elsevier B.V. All rights reserved.
doi:10.1016/j.jhazmat.2008.07.109

it attractive as a stable electrode to electro-generate hydrogen peroxide by the reduction of O_2 on its surface [21–23]. However, the electro-Fenton process based on ACF and Fe^{2+} still encounters the problems of acidic pH requirement (pH 2–4) and high amount of iron sludge in the coagulation step. These problems may be avoided by the utilization of heterogeneous Fenton reagents such as metal oxides [24] and some combined technology had been reported to overcome the narrow pH of the E-Fenton process [25,26].

Recently, we synthesized Fe@Fe_2O_3 core–shell nanowires simply by the reduction of Fe^{3+} ions with sodium borohydride in aqueous solution at ambient conditions [27]. These Fe@Fe_2O_3 core–shell nanowires were used as an iron reagent to efficiently degrade rhodamine B (RhB) in a sono-Fenton system at pH 2 [28]. Meanwhile, we found that the Fe@Fe_2O_3 core–shell nanowires could be as the iron reagent in the Fenton system to extend the working pH range and prevent the coagulation of iron ions [29]. Moreover, we combined core–shell Fe@Fe_2O_3 nanowires and multiwall carbon nanotubes (CNTs) by using poly-tetrafluoroethylene (PTFE) to fabricate an oxygen-fed gas diffusion electrode. We interestingly found the resulting Fe@Fe_2O_3/CNTs composite electrode was able to degrade dye pollutant at neutral pH [30]. Because of its excellent adsorption, ACF can easily adsorb iron ions. The subsequent reduction of iron ions on the ACF by $NaBH_4$ could result in a Fe@Fe_2O_3/ACF composite electrode.

In this study, we loaded nanostructured Fe@Fe_2O_3 on ACF to fabricate a Fe@Fe_2O_3/ACF composite electrode and then designed a novel heterogeneous E-Fenton system with this composite electrode. In this heterogeneous E-Fenton system, Fe@Fe_2O_3 and ACF were used as a controllably releasing Fenton iron reagent and an air-fed cathode to electro-generate H_2O_2, respectively. We chose rhodamine B as a model refractory organic pollutant to test the performance of this novel heterogeneous E-Fenton system. It was found that this heterogeneous E-Fenton system with the Fe@Fe_2O_3/ACF cathode showed much higher activity than other E-Fenton systems with commercial zero valent iron powders (Fe^0) and ferrous ions (Fe^{2+}) under neutral pH. The heterogeneous E-Fenton system with the Fe@Fe_2O_3/ACF cathode can enlarge the using pH scale of Fenton reaction.

2. Experimental

2.1. Chemicals

Sodium sulfate anhydrous, ferric chloride, sodium borohydride, sulfuric acid, reduced iron powder and other chemical reagents were all of analytical grade and purchased from Shanghai Chemical Reagents Company. All chemicals were used as received without further purification. Active carbon fiber (ACF) and titanium mesh were purchased from China Southern Chemicals Import and Export Corporation. Doubly distilled water was used in all experiments.

2.2. Preparation of the Fe@Fe_2O_3/ACF composite cathode

The composite cathode was prepared by loading Fe@Fe_2O_3 on ACF as follows. A 0.3 g amount of $FeCl_3{\cdot}6H_2O$ was dissolved in 100 mL of distilled water to obtain a ferric solution. A 0.6 g amount of $NaBH_4$ was dissolved in 40 mL of distilled water to get a $NaBH_4$ solution. After 20 min's sonication of ACF (1.5 cm × 2 cm) in the resulting ferric solution, the $NaBH_4$ solution was dropped to reduce ferric ions into metallic iron on ACF. The Fe@Fe_2O_3/ACF composite electrode was washed with deionized water thoroughly and then dried in nitrogen for further use. The quantity of Fe loading on the ACF was measured by weight method and kept 0.1 g L^{-1} of Fe@Fe_2O_3 in the final solution in each experiment. The Fe@Fe_2O_3/ACF composite electrode was fixed with titanium mesh before use. For comparison, ACF was also used as the cathode in the presence of 0.1 g L^{-1} of commercial Fe^0 and Fe^{2+} in the solution, which were denoted as Fe^0/ACF and Fe^{2+}/ACF, respectively.

2.3. Characterization of the Fe@Fe_2O_3/ACF electrode

The morphology of the Fe@Fe_2O_3/ACF electrode was characterized using X-ray diffraction (XRD) with Cu Kα radiation (Bruker D8 Advance), scanning electron microscopy (SEM, JSM-5600LV) with an accelerating voltage of 20 kV and transmission electron microscope (TEM, Philips CM-120) with an accelerating voltage of 200 kV. The element analysis of Fe@Fe_2O_3/ACF electrode was characterized by energy dispersive X-ray spectroscopy (EDX, 1530 VP Ger. LEO with OXFORD INCA-300) connected to the SEM. The elemental mapping was performed using a Gatan image filtering (GIF) system attached to a Tecnai 20 FEG transmission electron microscope. For the TEM analyses, the sample was sonicated in ethanol. Two drops of suspension were then dropped onto a carbon-coated copper grid.

2.4. Degradation of rhodamine B

E-Fenton degradation of RhB was preformed in a divided thermostatic cell with a two-electrode system that has been reported in our previous work [31], by using a CHI-660B (Shanghai, China) electrochemical workstation. A Pt sheet (99.99% purity, Beijing Academy of Steel Service) of 2.0 cm^2 in area was used as the anode. The as-prepared Fe@Fe_2O_3/ACF electrode was the cathode. The initial concentration of RhB was 5 mg L^{-1}. 0.05 mol L^{-1} of Na_2SO_4 aqueous solution was used as the electrolyte to increased the conductivity. The initial pH of the RhB solution was neutral at 6.2. In some cases, 0.5 mol L^{-1} of NaOH or H_2SO_4 were used to adjust the pH of the RhB solution. A 5 L min^{-1} of fresh air was fed to the cathode. The solution was magnetically stirred at room temperature during the whole E-Fenton reaction. Before degradation experiments, the system was stirred for 30 min to establish adsorption/desorption equilibrium between the solution and electrodes in the cathodal cell. As a comparison, E-Fenton processes with pure ACF electrode alone, and 0.1 g L^{-1} of commercial Fe^0 and ACF, 0.1 g L^{-1} of Fe^{2+} and ACF (denoted as ACF, Fe^0/ACF and Fe^{2+}/ACF, respectively) were conducted under the same conditions, respectively. The concentration of RhB was monitored by colorimetry with a U-3310 UV–vis spectrometer (HITACHI) at an interval of 20 min. The chemical oxygen demand (COD) was determined by the potassium dichromate method.

2.5. Determination of hydrogen peroxide and total iron ions concentrations

The analysis of hydrogen peroxide produced the solution was carried out with triiodide method using the UV–vis spectrum and off-line sampling [32]. The concentration of total iron ions (Fe^{2+} and Fe^{3+}) in the solution was measured by atom absorption spectrometry (WFX-1F2, China) [33].

3. Results and discussion

3.1. Characterizations of the resulting Fe@Fe_2O_3/ACF electrode

XRD pattern reveals the existence of cubic Fe (JCPDS, file No. 06-0696) in the as-prepared electrode (Fig. 1). The morphologies of the ACF and as-synthesized composite electrode were investigated by SEM. The original ACFs are about 4–6 μm in diameter and several tens to hundreds micrometers in length (Fig. 2a). Fig. 2b

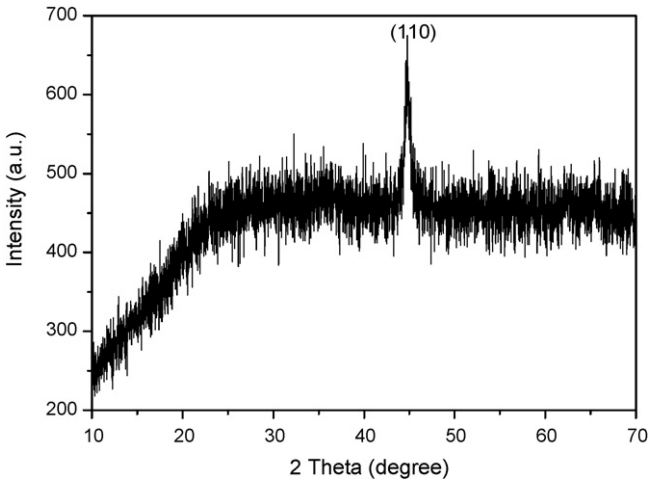

Fig. 1. XRD pattern of the as-prepared composite electrode before being using as the cathode in the E-Fenton reaction process.

shows that nanostructured iron was successfully loaded on ACF. High magnification SEM image displays that these nanostructured iron are mainly spheres with 10–100 nm in diameter (left inset of Fig. 1b), different from the nanowire structures obtained in our previous studies [27]. This indicates that the presence of ACF inhibits the magnetic self-assembly of nanospheres to nanowires. Energy dispersive X-ray analysis confirms the coexistence of Fe, C and O in the composite electrode (right inset of Fig. 2b). The morphology of nanostructured iron was further investigated by TEM. Chainlike nanoparticles or randomly aggregated nanoparticles were observed in the TEM images (Fig. 3). Meanwhile, some nanowires could also be found. The results of elemental mapping of Fe and O of the nanoparticles in the composite cathode confirmed the iron core and iron oxide shell structure of the nanoparticles (Fig. 3). The reason for no Fe_2O_3 in XRD patterns is because that these Fe_2O_3 shells were amorphous or that their sizes were too small to be detected by XRD. These phenomena were observed in our previous work [29]. This result is consistent with Liu's report, in which the particles have a core/shell structure with a shell thickness of 5–6 nm and they are poorly ordered or amorphous [34]. On the basis of the above results and reports, we conclude that the as-prepared composite electrode is ACF loaded with core–shell $Fe@Fe_2O_3$.

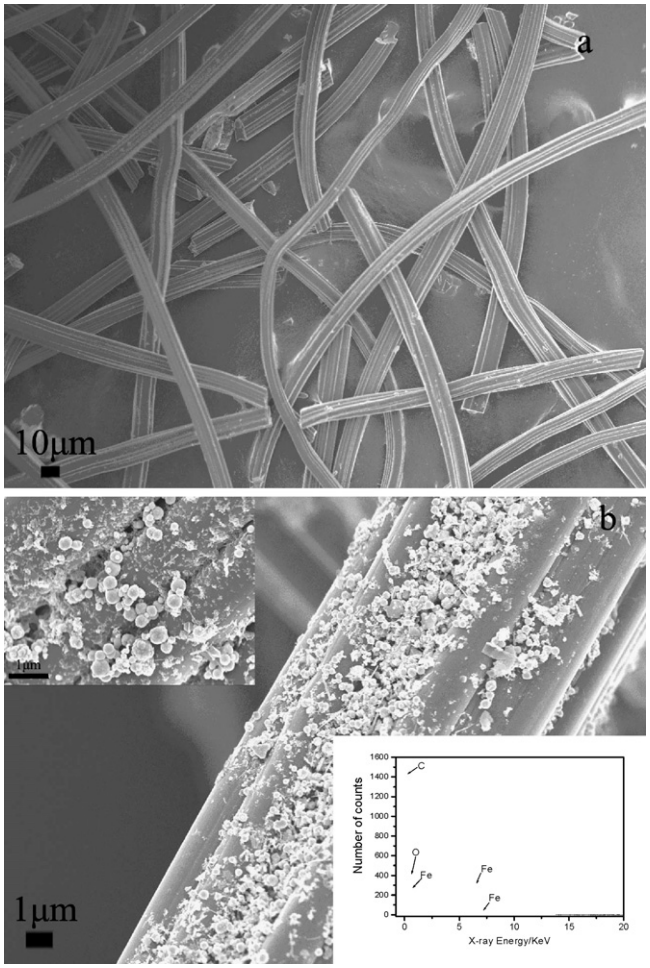

Fig. 2. The SEM images of the ACF (a) and as-prepared $Fe@Fe_2O_3$/ACF electrodes (b). The left and right insets of Fig. 1b are high magnification SEM image and energy dispersive spectrum of the as-prepared $Fe@Fe_2O_3$/ACF electrodes, respectively.

3.2. The E-Fenton degradation of RhB

In the traditional Fenton oxidation process (Fe^{2+}/H_2O_2), the optimal working pH value of the solution is 2–3. The oxidative capability of the Fenton system is weak if pH > 4 [35–38]. Therefore, it is of great importance to extend the Fenton reaction to efficiently work at neutral pH. Fig. 4 shows the degradation of RhB in various E-Fenton processes at neutral pH. Without any Fenton iron reagents, the electrochemical degradation of RhB on ACF electrode was merely 10% in 120 min. While the degradation of RhB in $Fe@Fe_2O_3$/ACF, Fe^0/ACF, and Fe^{2+}/ACF E-Fenton processes were 74.1%, 47.6%, and 25.5% in 120 min at neutral pH, respectively. These comparisons reveal high activity of $Fe@Fe_2O_3$/ACF E-Fenton system at neutral pH.

UV–vis spectra change of RhB is able to clarify the degradation mechanism of RhB in $Fe@Fe_2O_3$/ACF E-Fenton process (inset of Fig. 4). The spectrum of RhB in water was characterized by one main band in the visible region with maximum absorption at 555 nm, and two bands in the ultraviolet region with peaks located at 250 and 350 nm. The latter two peaks were ascribed to the absorption of the Π–Π^* transition related to the xanthenic rings bonded the —C=C— group in the dye molecule. The band in visible region was attributed to the ethyl containing azo linkage of the dye molecules. The absorption peak at λ = 555 nm diminished in the $Fe@Fe_2O_3$/ACF E-Fenton process, indicating a rapid degradation of RhB by breaking ethyl containing azo linkage. This decrease was very meaningful for the removal of azo dyes with the —N=N— bonds. The intensity of absorption at 250 and 350 nm also gradually decreased during the E-Fenton treatment, which indicated the destruction of the naphthalene rings [39].

3.3. The analysis of H_2O_2 and iron ions in the reaction solution

Because both H_2O_2 and iron ions are the crucial regents to produce •OH for the degradation of RhB in Fenton reaction, we measured the concentrations of hydrogen peroxide and iron ions produced during the RhB degradation in $Fe@Fe_2O_3$/ACF E-Fenton process at different pH. Fig. 5 shows the concentration of H_2O_2 in the bulk solution during the $Fe@Fe_2O_3$/ACF E-Fenton process at neutral pH and acidic conditions (pH 2–3). The H_2O_2 concentration increased with extending the reaction time. After approximately 90 min reaction, the accumulated H_2O_2 reached a steady state and did not increase any more. This indicates a balance between the decomposition and production of the hydrogen peroxide in the cathodal cell. In this steady state, H_2O_2 was electro-generated

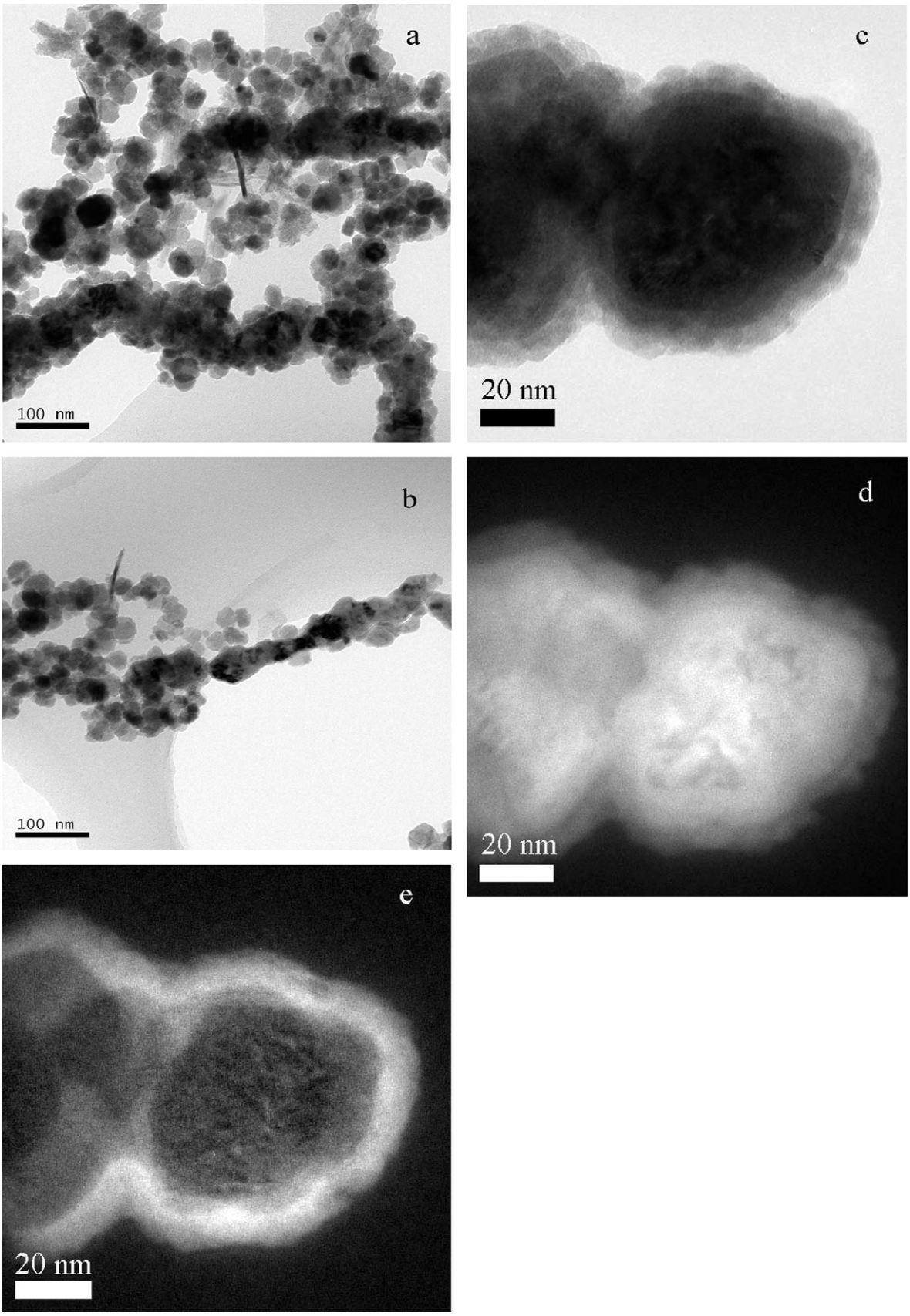

Fig. 3. The TEM images (a and b) and elemental mappings (c and d) of the as-prepared Fe@Fe_2O_3 nanostructures in the Fe@Fe_2O_3/ACF electrode. (c) Original TEM image; (d) mapping of Fe in (c); (e) mapping of O in (c).

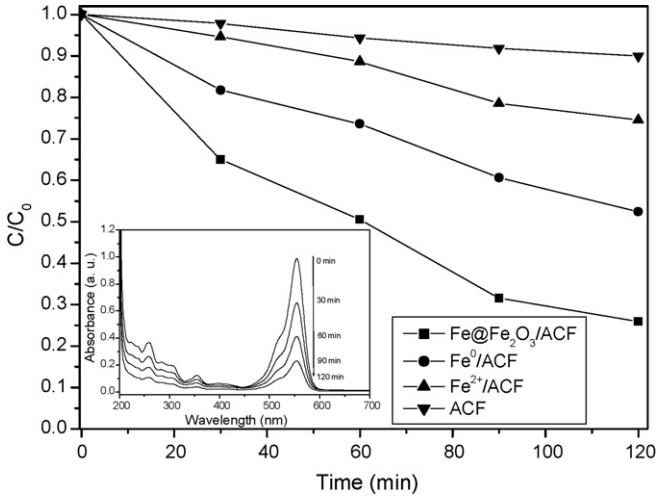

Fig. 4. Degradation of RhB in different E-Fenton processes with a two-electrode system at neutral pH. The inset is UV–vis spectra changes of RhB in the Fe@Fe_2O_3/ACF E-Fenton process. The applied potential between the cathode and the anode was −1.2 V, the electrolyte was 0.05 mol L^{-1} of Na_2SO_4, the initial concentration of RhB was 5 mg L^{-1}.

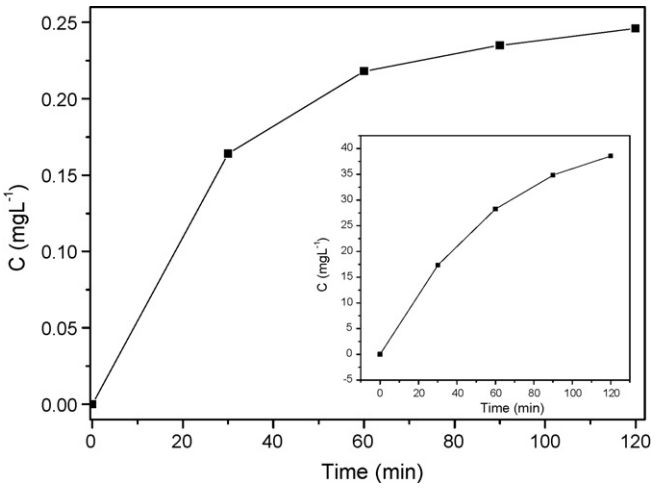

Fig. 6. Time-course of iron concentrations during the Fe@Fe_2O_3/ACF E-Fenton degradation of RhB at neutral pH and pH 2–3 (inset) with a two-electrode system. The applied potential between the cathode and the anode was −1.2 V, the electrolyte was 0.05 mol L^{-1} of Na_2SO_4, the initial concentration of RhB was 5 mg L^{-1}.

and simultaneously consumed in the system at the same rate. As a comparison, the production of H_2O_2 under an acidic condition was also detected (inset of Fig. 5). The produced H_2O_2 at pH 2–3 was less than that at neutral pH. Meanwhile, the concentrations of iron ions leached from the Fe@Fe_2O_3/ACF composite electrode to the RhB solution at various pH values were determined by atom absorption spectrometry (Fig. 6). The concentration of iron ions after 120 min of RhB degradation in the Fe@Fe_2O_3/ACF E-Fenton process was very low (only 0.246 mg L^{-1}) at neutral pH, much lower than that (about 38 mg L^{-1}) at acidic pH (inset of Fig. 6). Moreover, during the Fe@Fe_2O_3/ACF E-Fenton degradation of RhB at neutral pH, the concentration of the iron ions only increase quickly at the beginning. However, after 60 min the concentration of the iron ions did not increase any more. The repeated experiments of the Fe@Fe_2O_3/ACF electrode for E-Fenton degradation of RhB (Fig. 7) confirmed that this Fe@Fe_2O_3/ACF electrode can be used for a long time and reusable.

The process of corrosion of Fe@Fe_2O_3 in the Fe@Fe_2O_3/ACF E-Fenton process at acid condition may be depicted by the following reaction at Eq. (6).

$$Fe + 2H^+ \rightarrow Fe^{2+} + H_2 \quad (6)$$

The corrosion of Fe@Fe_2O_3 at neutral pH becomes very slowly (Fig. 6). It is known that the optimum acidity for Fe^{2+} ions to catalyze the decomposition of hydrogen peroxide (Eq. (2)) is pH 2–3. However, in the electrolysis system, the optimum condition for the electro-generation of hydrogen peroxide is in basic solution, especially at pH 10–11 [40]. Obviously, these two requirements cannot meet well at the same time. This is the reason for the low efficiency of Fe^{2+}/ACF system. Interestingly, we found that the RhB degradation efficiency of the Fe@Fe_2O_3/ACF E-Fenton process was not significantly affected by the solution pH (Fig. 8). Actually, the residual concentration of rhodamine B increased with increasing pH, because the Fenton reactions take place more easily at acid pH value than that at basic pH. In the Fig. 8, we think the RhB can be degraded in the pH 2–10 despite of the degradation in the

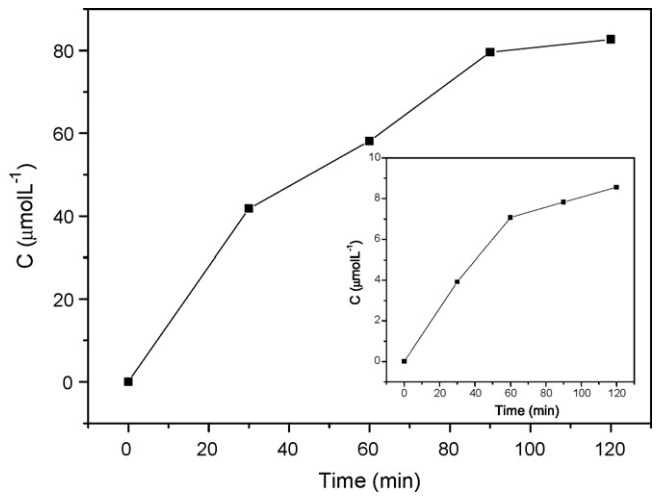

Fig. 5. Time-course of H_2O_2 concentrations during the Fe@Fe_2O_3/ACF E-Fenton degradation of RhB at neutral pH and pH 2–3 (inset) with a two-electrode system. The applied potential between the cathode and the anode was −1.2 V, the electrolyte was 0.05 mol L^{-1} of Na_2SO_4, the initial concentration of RhB was 5 mg L^{-1}.

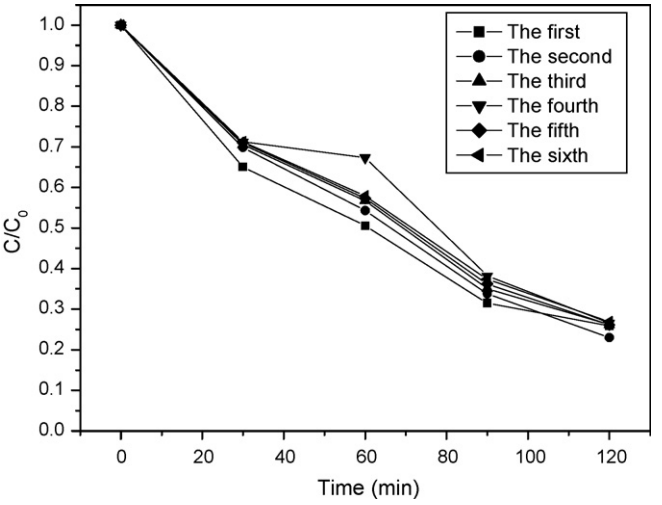

Fig. 7. The recycle experiments of Fe@Fe_2O_3/ACF electrodes for E-Fenton degradation of RhB. The applied potential between the cathode and the anode was −1.2 V, the electrolyte was 0.05 mol L^{-1} of Na_2SO_4, the initial concentration of RhB was 5 mg L^{-1}.

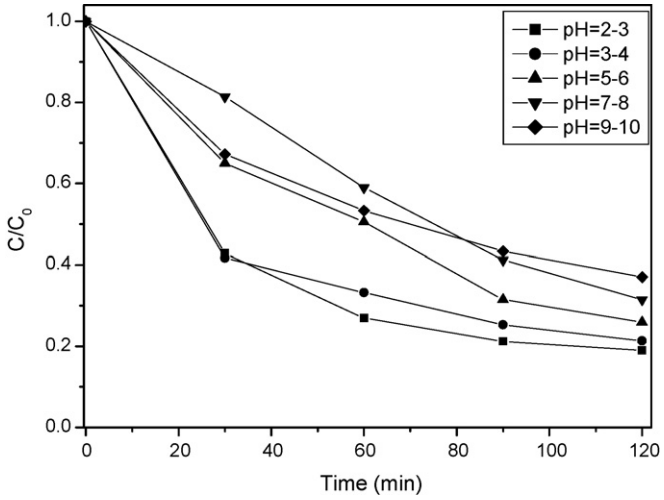

Fig. 8. Influence of solution pH on the RhB degradation in the Fe@Fe_2O_3/ACF E-Fenton process. The applied potential between the cathode and the anode was −1.2 V, the electrolyte was 0.05 mol L^{-1} of Na_2SO_4, the initial concentration of RhB was 5 mg L^{-1}.

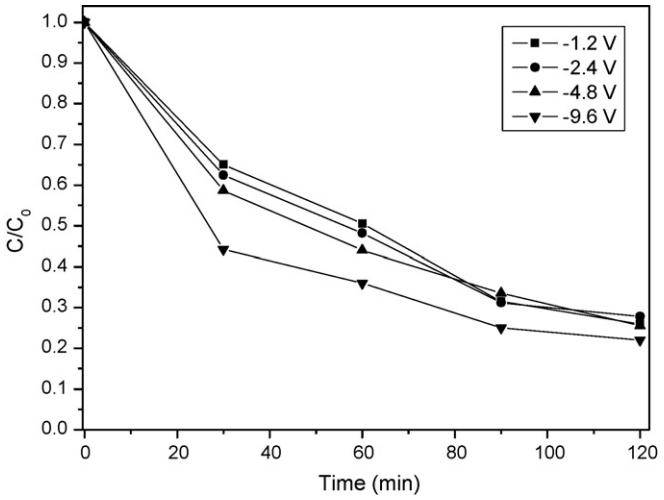

Fig. 9. Influence of applied potential between the cathode and the anode on the RhB degradation in the Fe@Fe_2O_3/ACF E-Fenton process. The electrolyte was 0.05 mol L^{-1} of Na_2SO_4, the initial concentration of RhB was 5 mg L^{-1}.

acid solution better than basic. Assuming that the RhB degradation reaction follows the pseudo-first-order kinetic model, the kinetic constants of Fe@Fe_2O_3/ACF E-Fenton degradation at different pH were calculated and summarized in Table 1. The kinetic constant at pH 2–3 was 0.013 min^{-1}. This value was very close to those under the neutral or basic conditions, although the produced iron ions at pH 2–3 was much more than that at neutral pH (Fig. 6). We also found that the pH went up to a basic pH when the initial pH was from acid pH to base pH, because the H^+ in solution was consumed through the reaction in Eqs. (1) and (6). This advantage makes this Fe@Fe_2O_3/ACF E-Fenton system feasible at higher pH value without sacrificing efficiency.

The influence of applied potential between the cathode and the anode on neutral pH Fe@Fe_2O_3/ACF E-Fenton degradation of RhB was examined at different cathodal voltages (−1.2, −2.4, −4.8, and −9.6 V) (Fig. 9). Similar to pH, applied potential did not significantly affect the efficiency of this novel E-Fenton system much. The pseudo-first-order kinetic constants were summarized in Table 2. The relationship between the production of •OH and the concentrations of Fe^{2+} and H_2O_2 is shown in Eq. (7), where λ is the coefficient of the E-Fenton reaction, k is the apparent rate constant of the E-Fenton reaction, $[Fe^{2+}]$ and $[H_2O_2]$ are the concentrations of iron ions and H_2O_2 produced in the E-Fenton process.

$$[\bullet OH] = \lambda \times \left(\frac{d[\bullet OH]}{dt}\right)_g \lambda \times k \times [Fe^{2+}] \times [H_2O_2] \quad (7)$$

According to Eq. (7), the increasing applied potential could enhance the production of electrogenerated H_2O_2. However, higher absolute applied potential would result in more parasitic reactions, such as electrolysis of water. These parasitic reactions would reduce efficiency. Therefore, the overall efficiencies of this system at different applied potentials are similar. Meanwhile, the current efficiency at different applied potential was calculated by using Eq. (8).

$$\mathrm{ICE} = \left[\frac{(\mathrm{COD})_0 - (\mathrm{COD})_t}{(8 \times I \times t) \times F \times V \times 100\%}\right] \quad (8)$$

where COD_0 and COD_t denote the original COD and COD measured at time of t, respectively; F is the Faraday constant (96 485 C mol^{-1}); V is the volume of the electrolyte (dm^{-3}); I is the current (A). In our reaction system, the total volume of the solution is not approximately changed. The current increases with increasing the applied potential. The current efficiencies of different applied potentials were summarized in the Table 2. It is obvious that higher absolute applied potential resulted lower current efficiency. Therefore, using lower absolute applied potential can save more energy in our Fe@Fe_2O_3/ACF E-Fenton system.

3.4. The E-Fenton degradation mechanism

On the basis of the above results, we proposed a possible pathway for the RhB degradation in the Fe@Fe_2O_3/ACF E-Fenton process under neutral pH (Scheme 1). First, oxygen was adsorbed on the surface of Fe@Fe_2O_3/ACF electrode and part of iron ions was leached into the solution at the same time. H_2O_2 was then formed by electro-chemically reduction of oxygen adsorbed on the composite electrode. In the next step, the leached iron ions would react with H_2O_2 to produce hydroxyl radicals. Finally, RhB was degraded by the produced hydroxyl radicals. Obviously, the core–shell structure of Fe@Fe_2O_3 is crucial for the high efficiency of this heterogeneous E-Fenton system in view of lower activity of the Fe^0/ACF E-Fenton system. According to our previous study [30], the core–shell structure could prevent the complete leaching of iron ions into the RhB solution because the formed iron ions

Table 1
Pseudo-first-order constants, the corresponding coefficients, and residual RhB after 120 min of degradation in the Fe@Fe_2O_3/ACF E-Fenton process at various pH

pH	Kinetic constant (min^{-1})	Coefficient (R^2)	Residual RhB (%)
2–3	0.013	0.8832	19.1
3–4	0.012	0.8823	21.3
5–6	0.011	0.9858	25.9
7–8	0.010	0.9931	31.5
9–10	0.010	0.9838	37.3

Table 2
Pseudo-first-order constants, the corresponding coefficients, residual RhB and current efficiency after 120 min of degradation in the Fe@Fe_2O_3/ACF E-Fenton process at various applied potentials between the cathode and the anode

Potential (V)	Kinetic constant (min^{-1})	Coefficient (R^2)	Residual RhB (%)	Current efficiency (%)
−1.2	0.011	0.9858	25.9	76.4
−2.4	0.011	0.9673	27.8	66.9
−4.8	0.011	0.9753	25.5	50.6
−9.6	0.012	0.9028	22.4	43.2

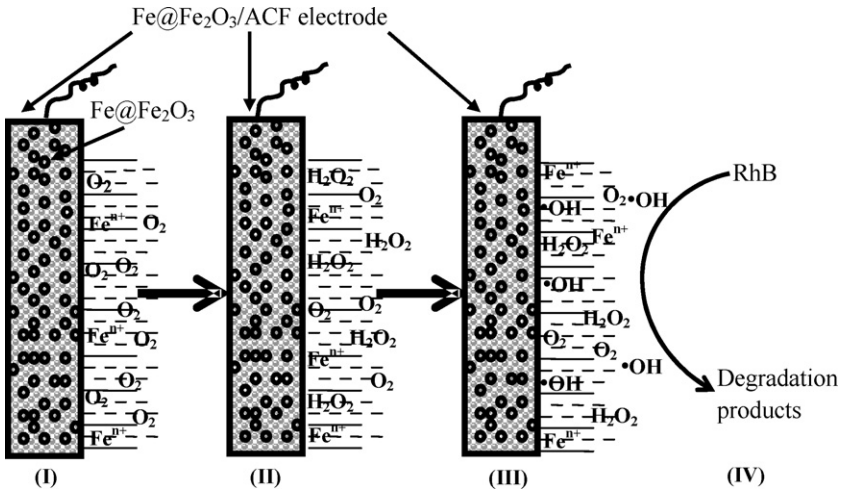

Scheme 1. Schematic illustration of RhB degradation in the Fe@Fe_2O_3/ACF E-Fenton process at neutral pH (pH 6.2). (I) Adsorption of oxygen on the surface of Fe@Fe_2O_3/ACF electrode and leaching of iron ions into the solution; (II) reduction of oxygen on the surface of Fe@Fe_2O_3/ACF electrode; (III) formation of hydroxyl radicals; (IV) degradation of RhB.

could be adsorbed by the oxide shell of Fe@Fe_2O_3. The presence of ACF may further prevent the leaching of iron ions. This controlled release of iron ions would realize an in situ recycling of iron species ($Fe^0 \rightarrow Fe^{n+} \rightarrow Fe_2O_3$) and produce a new iron reagent containing iron ions, zero valent iron and iron oxides (Fe_2O_3). This new iron reagent served as a heterogeneous iron catalyst to catalyze the decomposition of the electro-generated H_2O_2 to generate hydroxyl radicals to attack RhB [30]. Therefore, this novel Fe@Fe_2O_3/ACF E-Fenton system showed good performance on the degradation of RhB at neutral pH. The application of this promising E-Fenton process to degrade other pollutants at neutral pH is in progress.

Acknowledgements

This work was supported by National Basic Research Program of China (973 Program) (Grant 2007CB613301), National Science Foundation of China (Grants 20673041 and 20503009), Open Fund of Key Laboratory of Catalysis and Materials Science of the State Ethnic Affairs Commission & Ministry of Education, Hubei Province (Grants CHCL0508 and CHCL06012), and Postdoctors Foundation of China (Grants 20070410935).

References

[1] W.R. Chen, C.M. Sharpless, K.G. Linden, I.H. Suffet, Treatment of volatile organic chemicals on the EPA contaminant candidate list using ozonation and the O_3/H_2O_2 advanced oxidation process, Environ. Sci. Technol. 40 (2006) 2734–2739.
[2] L. Yong, K.C. Armstrong, R.N. Dansby-Sparks, N.A. Carrington, J.Q. Chambers, Z.L. Xue, Quantitative analysis of trace chromium in blood samples. Combination of the advanced oxidation process with catalytic adsorptive stripping voltammetry, Anal. Chem. 78 (2006) 7582–7587.
[3] H. Destaillats, A.J. Colussi, J.M. Joseph, M.R. Hoffmann, Synergistic effects of sonolysis combined with ozonolysis for the oxidation of azobenzene and methyl Orange, J. Phys. Chem. A 104 (2000) 8930–8935.
[4] M.O. Buffle, G.V. Gunten, Phenols and amine induced HO• generation during the initial phase of natural water ozonation, Environ. Sci. Technol. 40 (2006) 3057–3063.
[5] K. Swaminathan, S. Sandhya, S.A. Caramlin, K. Pachhade, Y.V. Subrahmanyam, Decolorization and degradation of H-acid and other dyes using ferrous-hydrogen peroxide system, Chemosphere 50 (2003) 619–625.
[6] I. Arslan, I.A. Balcioglu, Degradation of remazol black B dye and its simulated dye bath wastewater by advanced oxidation processes in heterogeneous and homogeneous media, Color. Technol. 117 (2001) 38–42.
[7] S. Meric, D. Kaptan, T. Olmez, Color and COD removal from wastewater containing reactive black 5 using Fenton's oxidation process, Chemosphere 54 (2004) 435–441.
[8] M. Muruganandham, M. Swaminathan, Decolourisation of reactive orange 4 by Fenton and photo-Fenton oxidation technology, Dyes Pigments 63 (2004) 315–321.
[9] P.K. Malik, S.K. Saha, Oxidation of direct dyes with hydrogen peroxide using ferrous ion as catalyst, Sep. Purif. Technol. 31 (2003) 241–250.
[10] F. Lücking, H. Köser, M. Jank, A. Ritter, Iron powder, graphite and activated carbon as catalysts for the oxidation of 4-chlorophenol with hydrogen peroxide in aqueous solution, Water Res. 32 (1998) 2607–2614.
[11] J.A. Zazo, J.A. Casas, A.F. Mohedano, M.A. Gilarranz, J.J. Rodriguez, Chemical pathway and kinetics of phenol oxidation by Fenton's reagent, Environ. Sci. Technol. 39 (2005) 9295–9302.
[12] C.L. Friedman, A.T. Lemley, A. Hay, Degradation of chloroacetanilide herbicides by anodic Fenton treatment, J. Agric. Food Chem. 54 (2006) 2640–2651.
[13] J. Yu, P.E. Savage, Reaction pathways in pentachlorophenol synthesis. 1. Temperature-programmed reaction, Ind. Eng. Chem. Res. 43 (2004) 5021–5026.
[14] M. Ogura, I. Astuti, T. Yoshikawa, K. Morita, H. Takahashi, Development of a technology for silicon production by recycling wasted optical fiber, Ind. Eng. Chem. Res. 43 (2004) 1890–1893.
[15] B. Boye, M.M. Dieng, E. Brillas, Degradation of herbicide-chlorophenoxyacetic acid by advanced electrochemical oxidation methods, Environ. Sci. Technol. 36 (2002) 3030–3035.
[16] M.A. Oturan, J. Peiroten, P. Chartrin, A.J. Acher, Complete destruction of *p*-nitrophenol in aqueousmedium by electro-Fenton method, Environ. Sci. Technol. 34 (2000) 3474–3479.
[17] B. Batanero, J. Escudero, F. Barba, Cathodal reduction of phenacyl azides, Org. Lett. 1 (1999) 1521–1522.
[18] N. Sano, T. Yamamoto, I. Takemori, S.I. Kim, A. Eiad-ua, D. Yamamoto, M. Nakaiwa, Degradation of phenol by simultaneous use of gas-phase corona discharge and catalyst-supported mesoporous carbon gels, Ind. Eng. Chem. Res. 45 (2006) 2897–2900.
[19] Y.H. Huang, S. Chou, M.G. Perng, G.H. Huang, S.S. Cheng, Case study on the bioeffluent of petrochemical wastewater by electro-Fenton method, Water Sci. Technol. 39 (1999) 145–149.
[20] J.P. Jia, J. Yang, J. Liao, W.H. Wang, Z.J. Wang, Treatment of dyeing wastewater with ACF electrodes, Water Res. 33 (1999) 881–884.
[21] P. Drogui, S. Elmaleh, M. Rumeau, A. Rambaud, Hydrogen peroxide production by water electrolysis: application to disinfection, J. Appl. Electrochem. 31 (2001) 877–882.
[22] E. Brillas, J. Casado, Aniline degradation by electro-Fenton and peroxi-coagulation processes using a flow reactor for wastewater treatment, Chemosphere 47 (2002) 241–248.
[23] E. Brillas, B. Boye, I. Sires, J.A. Garrido, R.M. Rodriguez, C. Arias, P.L. Cabot, C. Comninellis, Electrochemical destruction of chlorophenoxy herbicides by anodic oxidation and electro-Fenton using a boron-doped diamond electrode, Electrochim. Acta 49 (2004) 4487–4496.
[24] H.H. Huang, M.C. Lu, J.N. Chen, Catalytic decomposition of hydrogen peroxide and 2-chlorophenol with iron oxides, Water Res. 35 (2001) 2291–2299.
[25] S. Parra, V. Nadtotechenko, P. Albers, J. Kiwi, Discoloration of azo-dyes at biocompatible pH-values through an Fe-histidine Complex immobilized on Nafion via Fenton-like processes, J. Phys. Chem. B 108 (2004) 4439–4448.
[26] X.Z. Li, H.S. Liu, Development of an E-H_2O_2/TiO_2 photoelectrocatalytic oxidation system for water and wastewater treatment, Environ. Sci. Technol. 39 (2005) 4614–4620.
[27] L.R. Lu, Z.H. Ai, J.P. Li, Z. Zhang, Q. Li, L.Z. Zhang, Synthesis and characterization of Fe-Fe_2O_3 core–shell nanowires and nanonecklaces, Cryst. Growth Des. 9 (2007) 349–354.

[28] Z.H. Ai, L.R. Lu, J.P. Li, L.Z. Zhang, J.R. Qiu, M.H. Wu, Fe@Fe_2O_3 core–shell nanowires as iron reagent. 1. Efficient degradation of rhodamine B by a novel sono-Fenton process, J. Phys. Chem. C 111 (2007) 4087–4093.
[29] Z.H. Ai, L.R. Lu, J.P. Li, L.Z. Zhang, J.R. Qiu, M.H. Wu, Fe@Fe_2O_3 core–shell nanowires as iron reagent. 2. An efficient and reusable sono-Fenton system working at neutral pH, J. Phys. Chem. C 111 (2007) 7430–7436.
[30] Z.H. Ai, T. Mei, M. Liu, J.P. Li, F.L. Jia, L.Z. Zhang, J.R. Qiu, Fe@Fe_2O_3 core–shell nanowires as iron reagent. 3. Their combination with CNTs as an effective oxygen-fed gas diffusion electrode in a neutral electro-Fenton system, J. Phys. Chem. C 111 (2007) 14799–14803.
[31] J.P. Li, L.R. Lu, Z.H. Ai, F.L. Jia, L.Z. Zhang, Efficient visible light degradation of rhodamine B by a photo-electrochemical process based on a Bi_2WO_6 nanoplates film electrode, J. Phys. Chem. C 111 (2007) 6832–6836.
[32] C. Konnann, D. Bahnemann, M.R. Hofmann, Photocatalytic production of H_2O_2 and organic peroxides in aqueous suspensions of TiO_2, ZnO, and desert sand, Environ. Sci. Technol. 22 (1988) 798–806.
[33] A.R. Kyriakos, G.V. Panayiotis, Comparative spectrophotometric determination of the total iron content in various white and red Greek wines, Food Chem. 82 (2003) 637–643.
[34] Y.Q. Liu, H. Choi, D. Dionysiou, G.V. Lowry, Trichloroethene hydrodechlorination in water by highly disordered monometallic nanoiron, Chem. Mater. 17 (2005) 5315–5322.
[35] J. Jeong, J. Yoon, pH effect on •OH radical production in photo/ferrioxalate system, Water Res. 39 (2005) 2893–2900.
[36] Z.Y. Cheng, Y.Z. Li, W.B. Chang, Kinetic deoxyribose degradation assay and its application in assessing the antioxidant activities of phenolic compounds in a Fenton-type reaction system, Anal. Chim. Acta 478 (2003) 129–137.
[37] G.P. Anipsitakis, D.D. Dionysiou, Degradation of organic contaminants in water with sulfate radicals generated by the conjunction of peroxymonosulfate with cobalt, Environ. Sci. Technol. 37 (2003) 4790–4797.
[38] B.A. Smith, A.L. Teel, R.J. Watts, Identification of the reactive oxygen species responsible for carbon tetrachloride degradation in modified Fenton's systems, Environ. Sci. Technol. 38 (2004) 5465–5469.
[39] J.M. Wu, T.W. Zhang, Photodegradation of rhodamine B in water assisted by titania films prepared through a novel procedure, J. Photochem. Photobiol. A: Chem. 162 (2004) 171–177.
[40] H. Kokichi, D.X. Sun, L. Richard, K. Yoshinori, F. Gabriel, The mechanism of the enhanced antioxidant effects against superoxide anion radicals of reduced water produced by electrolysis, Biophys. Chem. 107 (2004) 71–82.